Smartphone App Brings Human Thermal Comfort Forecast in Your Hands

B. G. Heusinkveld, G. Sterenborg, G. J. Steeneveld, J. J. Attema, R. J. Ronda, and A. A. M. Holtslag

What activity would you consider doing tomorrow if the weather forecast predicts a temperature of 27°C? Taking your kids or grandparents for a walk, or maybe a good opportunity to visit that new art museum? That walk may become stressful if it is sunny and the path offers little shade along the way. However, on a windy day, or on a route shaded from direct sunlight, such as a narrow street canyon, thermal conditions may be just fine. By utilizing expert knowledge of the combined effects of temperature, humidity, wind speed, and radiation on the human thermal energy balance, it is possible to refine the general forecast to be more site specific about human comfort while outdoors. Climate change (McCarthy et al. 2010, Coumou and Rahmstorf 2012, Coumou and Robinson 2013), urbanization-related heating [the urban heat island effect (UHI)], and recorded excess mortality during recent European heat waves generated an acute awareness for heat-related health risks. The elderly, people with cardiovascular diseases, and outdoor workers are particularly vulnerable (Zander et al. 2015). Accordingly, the need for easily accessible and local forecasting of human thermal comfort is growing. This paper presents a new smartphone app that communicates a location-specific human thermal comfort forecast based on the latest innovations in urban climate and biometeorology, computer science, communication technology, and land-use mapping. The forecasts were evaluated against four years of observations in the Netherlands.

Humans are relatively limited in physiological thermoregulation strategies to cope with heat or cold and must rely on choice of clothing, shelter, or behavioral thermoregulation. Such strategies may also affect the choice of outdoor activities. A person's interpretation of a standard weather forecast is subjective, and various empirical thermal indices to enhance weather forecasts have been introduced. These include the wind chill factor (Osczevski and Bluestein 2005) to quantify wind speed effects on the severity of cold weather conditions and the heat index (Steadman 1979) for hot conditions coupled with the effect of humidity on a perceived temperature scale. Unfortunately, none of these empirical indices build upon a physically sound human thermal energy balance model, and site-specific information, as introduced by urban morphology, has been neglected.

Human thermal energy balance modeling has resulted in an "apparent" temperature that combines weather conditions, such as temperature, humidity, wind speed, and radiation. The latest insights are represented in the universal thermal climate index (UTCI) (Blzejczyk et al. 2012, Bröde et al. 2012). The UTCI is favored because it marries a dynamic clothing model and a state-of-the-art thermophysiological model of human heat transfer and temperature regulation (Fiala et al. 2012). The dynamic clothing model is based on what a person would wear according to the outdoor temperature (Havenith et al. 2012). The total human radiation load as part of the human thermal energy balance is expressed by a single temperature known as the mean radiant temperature T_{mrt} [Fanger 1970; see also sidebar "UTCI and mean radiant temperature T_{mrt}"].

The UTCI covers the full thermal exposure range

AFFILIATIONS: Heusinkveld, Sterenborg, Steeneveld, Ronda, and Holtslag—Meteorology and Air Quality Section, Wageningen University, Wageningen, Netherlands; Attema—Netherlands eScience Center, Amsterdam, Netherlands
CORRESPONDING AUTHOR: Bert Heusinkveld, bert.heusinkveld@wur.nl

DOI:10.1175/BAMS-D-16-0082.1

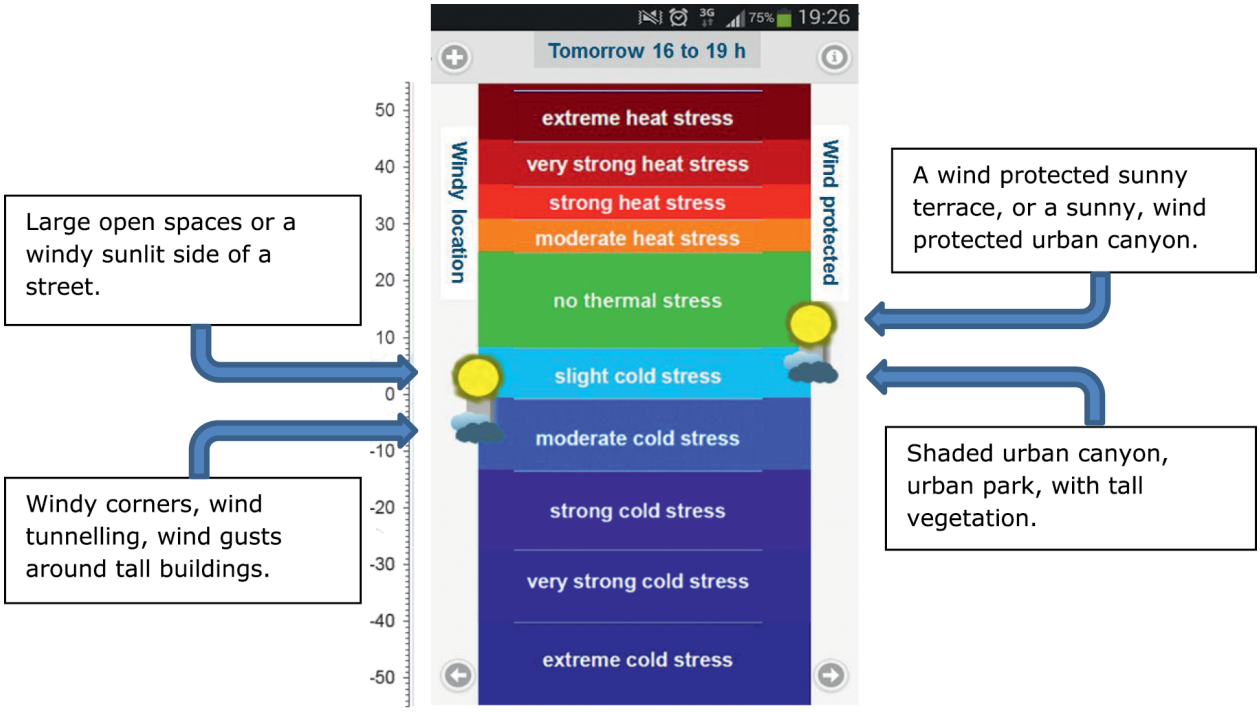

Fig. 1. App screen view of thermal stress levels on a 10-point scale according to the UTCI index. The time interval is given at the top of the screen. Text boxes on the sides present urban microclimate examples and show where to read their thermal forecasts from the app screen. The scale bar (not in the app) represents the UTCI temperature (°C).

(i.e., both cold and heat exposure) and is categorized into a basic 10-class human thermal stress scale. The forecast level of thermal exposure is presented by a color code and forms the basis for our smartphone app (Fig. 1). This allows for communication of thermal conditions using simple descriptive words such as "extreme heat stress" or "moderate cold stress" [see sidebar "UTCI and mean radiant temperature T_{mrt}"]. The UTCI was further tested across a range of climates from arctic to desert conditions and, over a range of thermal indices, the UTCI was best able to represent thermal stress levels (Blazejczyk et al. 2012).

Human thermoregulation is capable of handling a certain thermal range very well, but outside the "no thermal stress" range and especially on the hot side, the scale can shift easily to the next stress level (see widths of thermal classes in Fig. 1). The small stress steps on the hot side are related to the limited adaptation that a clothing change can offer, since clothing is most effective in the cold range. Because the UTCI standardizes the human being (body, dynamic clothing, metabolic rate, etc.), there is still some translation required to make a personalized judgment (fitness level, age, exercise intensity, etc.); however, using UTCI is more straightforward than using standard weather forecast data. Note that precipitation is not included in the human thermal energy balance and clothing model for the UTCI. The impact of wind and radiation on the UTCI is large, and therefore we consider it a great step forward to use a combination of high-resolution numerical weather prediction (NWP) and geoinformation to improve a standardized human thermal stress forecast.

Figure 2 illustrates the range of the UTCI classes (–29° to 40°C) on the basis of 4 years of observations (September 2011–September 2015) covering typical winter and summer weather conditions at the Veenkampen weather station in Wageningen, Netherlands (www.maq.wur.nl) (51.9809°N, 5.6197°E), which is a centrally located and representative weather station for the Netherlands. The station is equipped with solar and thermal radiometers (first class) mounted on a sun-tracker platform for direct, diffuse, and reflected solar radiation, and incoming thermal and shortwave radiation is measured separately. This

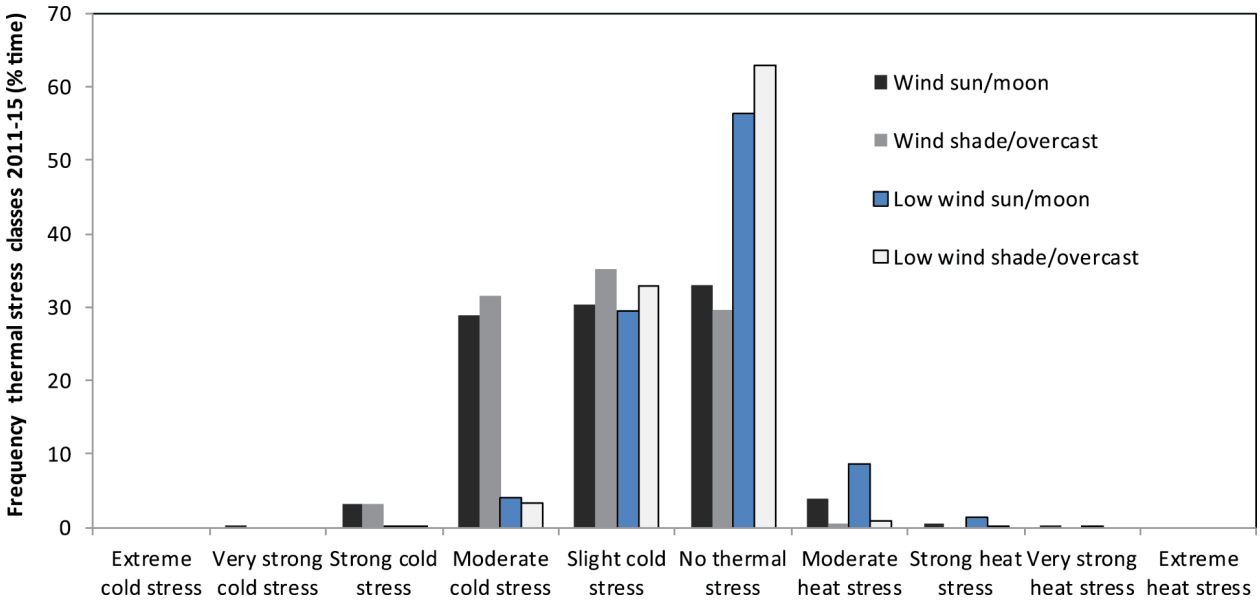

Fig. 2. Frequency distribution (%) of the observed maximum thermal stress class (September 2011–September 2015; all day, calculated for 3-h intervals).

allows for direct calculation of T_{mrt}. In this maritime temperate rural climate (Köppen class: Cfb), the UTCI is skewed toward cold stress conditions, and extreme UTCI classes do not occur. It is also seen that wind-protected or sunny locations increase heat stress classes.

Considering numerical weather forecasts, a tremendous increase in diversity, availability, and frequency of weather forecast communications has emerged. These communications now include newspapers, radio, television, text messaging, Internet, and smartphones. The number of products as derived from NWP models has increased accordingly. The demand ranges from nowcasting to short- and medium-range seasonal and climatological forecasting. This has generated new services that include drought, fire risk, and flooding. Currently, where smartphones have become a major tool for communication, planning, and weather updates, they are also excellent tools to access a *location-specific* weather forecast.

Advances in NWP represent a quiet revolution because the improvements were gradual, based on scientific and technological advances (Bauer et al. 2015). Typical NWP models are already performing very well when benchmarked against World Meteorological Organization (WMO) stations. The models are usually biased toward rural regions because NWP models have been optimized through data assimilation and model verification using WMO weather stations in rural locations. Current NWP models lack the resolution to resolve complex environments, such as cities. However, urbanized areas experience microclimates that differ greatly from rural settings (Oke 1982). A smartphone, however, knows its location and therefore can request very location-specific forecasts that may better suit user needs.

A similar increase in forecast skill can be expected by exploiting recent advances in geoinformation mapping. In the Netherlands, geoinformation (open-access) databases are regularly updated: lidar altimetry measurements with a density of more than 4 points per square meter and an accuracy of less than 0.1 m (www.ahn.nl), multispectral-band aerial photographs (resolution <0.5 m; Aerodata, Belgium), monthly vegetation index classification through satellite monitoring if cloud cover permits (www.groenmonitor.nl), and up-to-date maps of buildings (www.kadaster.nl). By combining these data, new products can be created, such as information about individual trees (www.boomregister.nl). Geoinformation data can also be converted to a high-resolution land-use and roughness map for high-resolution mesoscale weather prediction (Attema et al. 2015).

Figure 3 shows a flowchart of the steps that lead to the site-specific thermal stress forecast, which

can easily be adapted for other locations and future developments. The refined site-specific forecast accounts for urban land use and morphology at 50-m spatial resolution, which is reflected in the raised temperature (UHI) and wind speed reduction by enhanced surface roughness. Here the point of departure is the forecast from the European Centre for Medium- Range Weather Forecasts (ECMWF), which provides temperature, wind speed, radiation, and humidity. Already-subtle differences in shaded versus sunlit sides of a street can shift thermal stress levels by one class on the UTCI scale (Weihs et al. 2012). As the resolution provided by the smartphone's global positional system device is too coarse to distinguish between shaded and sunlit locations by the app itself, the app user determines one of the relevant environments at hand. A similar approach was adopted to estimate the impact of wind speed reduction. A shaded location is defined as a location with T_{mrt} equivalent to air temperature; such values are typical for narrow urban canyons. The sunny location is approximated by direct solar radiation and reduced diffuse radiation components. The thermal

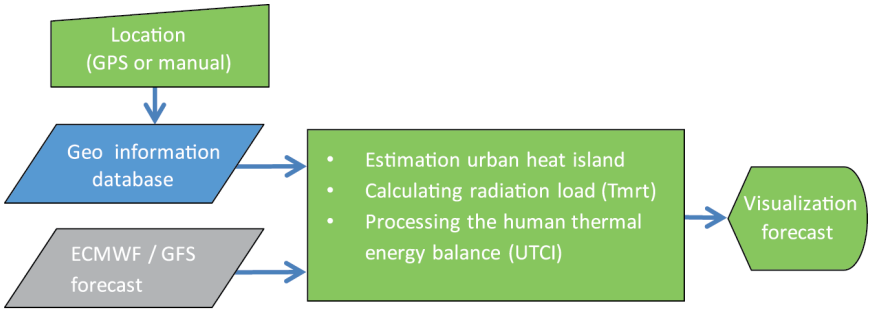

Fig. 3. Flowchart of human thermal comfort forecast calculations, data communications, and resources for the smartphone app (green: smartphone; blue: server at university; gray: NWP model).

UTCI AND MEAN RADIANT TEMPERATURE T_{MRT}

The universal thermal climate index was developed by a European Cooperation in Science and Technology working group known as "Thermophysiological Modeling and Testing Toward a Universal Thermal Climate Index for Assessing the Thermal Environment of the Human Being" [European Cooperation in Science and Technology (COST) Action 3730].

The UTCI is an equivalent temperature of an actual complex microclimate thermal condition incorporating temperature, humidity, wind speed, and solar and thermal radiation. The UTCI is the air temperature T_a of a reference condition causing the same dynamic physiological response (after a 30–120-min exposure) as experienced in a complex microclimate. These reference conditions include exercise intensity equivalent to walking 4 km h^{-1}, $T_{mrt} = T_a$, wind speed = 0.35 m s^{-1} (at 1.2 m), and relative humidity = 50% ($T < 29$°C) or vapor pressure = 2 kPa ($T > 29$°C).

The UTCI is calculated from a multinode (e.g., core, upper or lower arm, hand, or foot) human thermal energy balance model. It considers the human thermal regulatory functions, such as vasoconstriction and vasodilation, sweat rate, and shivering. A human being is standardized for the UTCI: surface area = 1.85 m^2, body weight = 73.4 kg, fat content = 14%, work load equivalent to walking 4 km h^{-1} [see Fiala et al. (2012) for further reading]. The UTCI assumes a dynamic clothing model and is based on what a person would wear according to the outdoor temperature (Havenith et al. 2012).

The UTCI equivalent temperature scale (°C) levels are a result of heat exchange with the environment caused by the physiological response of a human in actual environmental conditions. This is expressed in terms of heat or cold stress in 10 "stress" classes. Note that the large UTCI temperature range of the neutral class (no thermal stress; Fig. 1) is related to the effectiveness of human thermoregulation and adaptation through dynamic clothing. The classes are more closely spaced in the hot range compared with the cold range because of the limited adaptation possibilities (e.g., through clothing).

For simplification, an approximation equation for the UTCI can be used but requires 10-m wind speed from an airport weather station (z_0 = 0.01 m) (Bröde et al. 2012). Note that if wind speed is available at 1.2 m, it must be projected to 10-m height to use this equation (regardless of the location, multiply by 1.44).

It is common in human thermal energy balance modeling to express the solar and thermal radiation load as a mean radiant temperature T_{mrt}. It is the average surface temperature (skin and clothing) balancing the average absorbed solar and thermal radiation. The value of T_{mrt} considers the shape of a human being and thus weighs radiation from the sides more than from above and below. Standardized are shortwave radiation absorption (0.7), emissivity (0.97), and radiation interception shape factors (0.22) from four sides and from above and/or below (0.06).

radiation exposure is a sky-view-factor-weighted average of the incoming thermal radiation and NWP surface thermal radiation. It is still a work in progress to further refine T_{mrt}, for example, with a radiative transfer model using environmental morphology from geoinformation data (e.g., Lindberg et al. 2008). However, more data on building albedo and emissivity are required. Similarly, we argue that a wind-protected location as an extreme value may have just a slight draft, and therefore the UTCI reference climate wind speed condition was chosen [0.35 m s^{-1} at pedestrian level; see sidebar "UTCI and mean radiant temperature T_{mrt}"]. Within cities, the wind-tunnel effect can greatly increase wind speed. As a rule of thumb, in the local climate zones of typical Dutch cities, a windy spot would be equivalent to the rural wind speed at pedestrian level (Bottema 1993).

The above approach is sufficient to provide a thermal comfort range only (through the four location pictograms in Fig. 1)—that is, for a sunny and calm environment, a sunny and windy environment, a shaded and calm environment, and a shaded and windy environment. As a consequence, the broad thermal range forecast represents the outer extremes for the thermal condition within the vicinity of the location. It does not present a normal distribution, and within a city this distribution may be shifted toward lower cold stress or higher heat stress because of

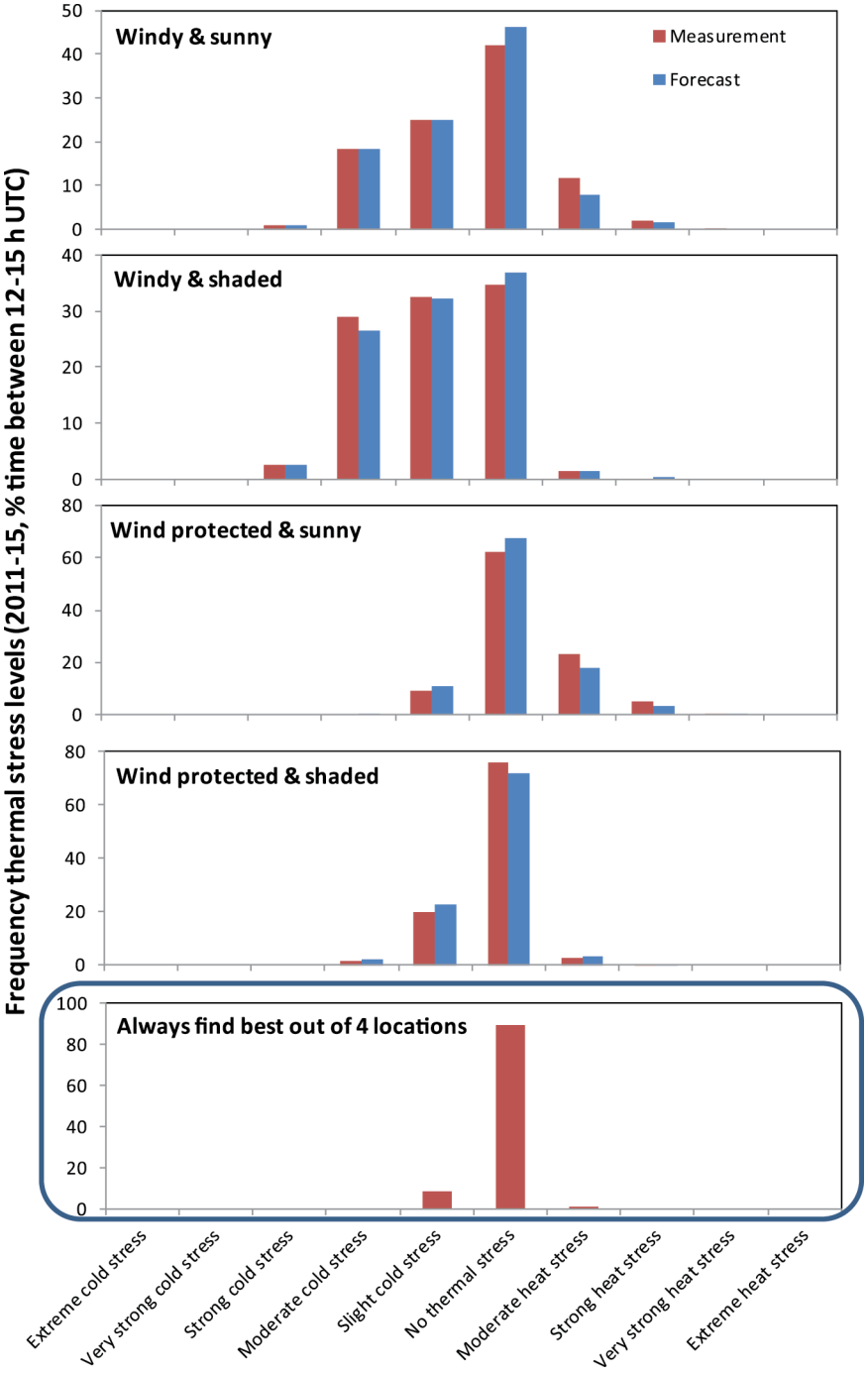

Fig. 4. (top four rows) Afternoon (1200–1500 UTC) thermal stress forecasts (+3-h lead) and measurements (in percentage of time) at four locations around the rural Wageningen University weather station and (bottom) a location based on minimization of thermal stress by always choosing the best forecast out of the top four locations (September 2011–September 2015).

wind speeds that are lower than at the rural weather station location. Measurement surveys using a meteorological-station-equipped bicycle revealed that the forecast of the UTCI is within the spatial range of the UTCI measurements around that forecast location (Heusinkveld et al. 2010).

The location-specific forecast can be interpreted along the color bar (Fig. 1). For a windy spot, the app user should look at the symbols on the left side, whereas for a wind-protected location, the user should look to the right side (Fig. 1). Note that the sun–moon symbol is representative of a more open sky, and during the night this can shift the sun–moon symbol below the cloud symbol (because of stronger thermal radiative heat loss to the sky).

Here we focus on the maximum stress class during daytime (1200–1500 UTC; time in the Netherlands is UTC plus 2 h in summer) and used a 4-yr evaluation of the forecast (Fig. 4). Obviously this time window greatly reduces the cold stress hours. We found that the majority of the daytime observations were in the "no thermal stress" class for the two low-wind categories. In the windy locations (Figs. 4a,b), the data were more skewed toward the cold side (compared with Figs. 4c,d). Strong heat stress occurs 5.5% of the time under wind-protected and sunny conditions (Fig. 4c, equivalent to 20 days yr^{-1}).

The histograms of wind-protected and sunny (Fig. 4c) and wind-protected and shaded locations (Fig. 4d) illustrate the impact of shading: it increases cold and reduces heat stress. This information can be used for behavioral thermoregulation, such as moving to a shady or windy spot if thermal conditions get too hot. Similarly, for cold stress, one would move to a sunny or calm spot. This adaptation strategy appears very effective, since by taking these interventions, thermal stress-free conditions are achieved in more than 90% of the cases or afternoons (Fig. 4e). We have assumed ideal cases, but in reality the windy location may be too far away, or the nearest shaded spot may have a higher amount of solar reflection or thermal emission from nearby surfaces that were not accounted for. Note that the frequency of hours with heat stress will roughly double in 2050 as compared to present-day climate (Molenaar et al. 2016).

For a windy and shaded location, there are almost no heat stress issues for the Netherlands. However, the situation differs within an urban environment where the daytime UHI may increase thermal stress levels. Measurements showed up to a 2-K increase for Rotterdam during daytime hot summer conditions (Heusinkveld et al. 2014). The nocturnal differences between urban and rural areas can be much larger and can be accounted for using high-resolution mesoscale models or by using a statistical downscaling model with a validated scaling framework (Theeuwes et al. 2017). Based on rural weather data, their scaling predicts the maximum UHI during the diurnal cycle. Next, the maximum UHI is scaled toward hourly values using the typical diurnal UHI cycle (Oke 1982).

The app forecast has been validated for all four possible microclimatic conditions (see examples in Fig. 1) at the rural Wageningen weather station. Within the 5-yr evaluation period, only 7 days were subject to missing data, and a nearby weather station provided data to fill the gaps (notably, days mostly without thermal stress). The forecast results appear to be better for cold stress classes because of the broader spacing of the classes on the cold side of the scale. Moreover, winter-season months have a relatively short daylight period, and thus direct radiation becomes a less important factor (Fig. 4).

For the statistical forecast evaluation, a multiclass contingency table was constructed. The Gandin–Murphy skill score (GMSS) was selected because this score can deal with more than two classes and weighs the model score for rare events relatively more strongly than for frequent events (Gandin and Murphy 1992). A score of 1 represents a perfect forecast, whereas 0 represents a random forecast (see sidebar "The Gandin–Murphy skill score"). In the Netherlands, only seven UTCI classes have been observed, and the extremes represent a very low frequency (Table 1). To have reliable statistics, the seven

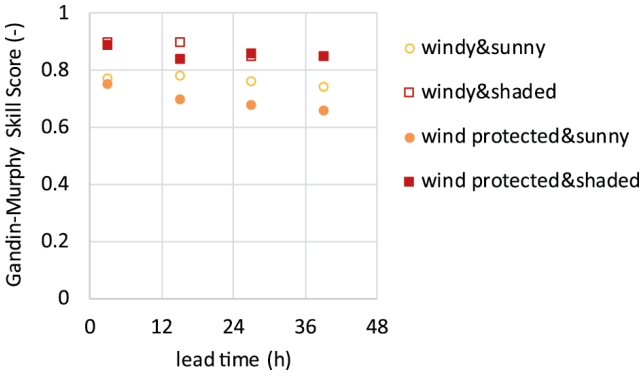

Fig. 5. Gandin–Murphy skill scores for a forecast of cold, neutral, or heat stress at four locations between 1200 and 1500 UTC (September 2011–September 2015).

		Observed						
		Strong cold stress	Moderate cold stress	Slight cold stress	No thermal stress	Moderate heat stress	Strong heat stress	Very strong heat stress
Forecast	Strong cold stress	7	7	0	0	0	0	0
	Moderate cold stress	5	221	42	0	0	0	0
	Slight cold stress	0	41	282	41	0	0	0
	Sum	**605**			**41**	**0**		
	No thermal stress	0	0	41	567	68	0	0
	Sum	**41**			**567**	**68**		
	Moderate heat stress	0	0	0	7	98	10	0
	Strong heat stress	0	0	0	0	3	20	1
	Very strong heat stress	0	0	0	0	0	0	0
	Sum	**0**			**7**	**132**		

Table 1. Contingency table for all thermal stress classes in Wageningen, Netherlands, for a windy and sunny location, number of afternoons (between 1200–1500 UTC 15 September 2011–15 September 2015; +3-h lead time). The sum rows represent the sum of cold, neutral, or heat stress classes. For example, the sum of the dark gray area (7) represents the observed cases of neutral conditions where heat stress was forecast.

THE GANDIN–MURPHY SKILL SCORE

Forecasts of weather events that occur infrequently (e.g., tornadoes, fog, and extreme precipitation) are usually evaluated using skill scores that are based on contingency tables in which combinations of correct forecasts and incorrect forecasts are recorded (Table 1). From the contingency table, skill scores like the hit rate, false-alarm rate, and critical success index have been well established for bimodal conditions for the forecasts and observations. However, for forecasts and observations that are organized in more than two categories, as in the app that uses multiple categories for human thermal comfort, a two-dimensional contingency table and its skill scores are not applicable. For multiple class forecasts, it is required that misses are scored analogous to single-class forecasts, though a skill score should preferably also account for the distance to the observed values and reward correct forecasts and penalize incorrect ones. Therefore, the Gandin–Murphy skill score (GMSS) was introduced. The GMSS first defines score weights for all available classes based on the sample climatology of the phenomenon of concern. Subsequently, these weights are applied to the joint probability of occurrence of each forecast–observation combination in the contingency table. As such, more credit is given to the correct forecast of rare events and less credit to correct forecasts of common events (Wilks 2006).

classes were regrouped into three categories—namely, cold stress, neutral, or heat stress (Table 1; see summation boxes). GMSSs are best (>0.84) for cases with shaded conditions (Fig. 5). Cloud cover appears to be more difficult to forecast than wind speed. This cloud cover issue is also evident in Table 1, which shows that the forecast has a cold bias in the heat stress classes only. The cold stress classes are dominated by wind effects, whereas the heat stress classes are dominated by radiation (and possibly related to seasonal changes in solar altitude). Note that a forecast lead time of 39 h reduces the GMSS only slightly.

One may also wonder what happens if only a rural UTCI forecast is used for all nearby microclimates. For a wind-protected location without shading, the rural UTCI forecast will underestimate heat stress, and this is clearly reflected in the GMSS; it drops from 0.70 to 0.47. For a shaded but not wind-protected location, the GMSS drops from 0.90 to 0.80. Surprisingly, for a shaded and wind-protected location, the score drops from 0.80 to 0.77 only. This is because of the categorization of GMSS in three groups. Overall, the added value of site-specific forecasts is significant.

In this paper we have introduced an app for forecasts of human thermal comfort and illustrated its performance for the Netherlands. We anticipate that future developments would benefit from increasingly improving geoinformation and higher-resolution weather forecasts (e.g., Ronda et al. 2017). Hopefully, readers are inspired to introduce similar apps for their environments and possibly link them to health risks caused by hypothermia, hyperthermia, air quality, and other effects (e.g., Steeneveld et al. 2017). The app was released in summer 2015 in the Netherlands and became very popular during the hot summer weather conditions. This is reflected in the number of users and forecast requests (around 300,000) during the first 2 weeks of operation.

In coming back to our initial question, yes, go ahead and find shade to avoid a strong heat stress class with the new tool at hand!

ACKNOWLEDGMENTS. The authors are grateful for funding from The Netherlands Organisation for Scientific Research (NWO)/eScience Grant 027.012.103. We appreciated advice by Kees Kok on the GMSS and extraction of ECMWF data by Folmer Krikken. Simon Berkowicz is thanked for his valuable input and proofreading. Finally, we thank ECMWF for making available their operational forecast archive.

FOR FURTHER READING

Attema, J. J., B. G. Heusinkveld, R. J. Ronda, G. J. Steeneveld, and A. A. M. Holtslag, 2015. Summer in the city: Forecasting and mapping human thermal comfort in urban areas. *IEEE 11th Int. Conf. on e-Science,* Munich, Germany, https://doi.org/10.1109/eScience.2015.21.

Bauer, P., A. Thorpe, and G. Brunet, 2015: The quiet revolution of numerical weather prediction. *Nature,* **525,** 47–55, https://doi.org/10.1038/nature14956.

Blazejczyk, K., Y. Epstein, G. Jendritzky, H. Staiger, and B. Tinz, 2012: Comparison of UTCI to selected thermal indices. *Int. J. Biometeorol.,* **56,** 515–535, https://doi.org/10.1007/s00484-011-0453-2.

Bottema, M., 1993: Wind climate and urban geometry. Ph.D. thesis, Dept. of Building physics, Eindhoven University, 211 pp.

Bröde, P., D. Fiala, K. Błażejczyk, I. Holmér, G. Jendritzky, B. Kampmann, B. Tinz, and G. Havenith, 2012: Deriving the operational procedure for the Universal Thermal Climate Index (UTCI). *Int. J. Biometeorol.,* **56,** 481–494, https://doi.org/10.1007/s00484-011-0454-1.

Coumou, D., and S. Rahmstorf, 2012: A decade of weather extremes. *Nat. Climate Change,* **2,** 491–496.

——, and A. Robinson, 2013: Historic and future increase in the global land area affected by monthly heat extremes. *Environ. Res. Lett.,* **8,** 034018, https://doi.org/10.1088/1748-9326/8/3/034018.

Fanger, P. O., 1970: *Thermal Comfort: Analysis and Application in Environment Engineering.* Danish Technical Press, 244 pp.

Fiala, D., G. Havenith, P. Brode, B. Kampmann, and G. Jendritzky, 2012: UTCI-Fiala multi-node model of human heat transfer and temperature regulation. *Int. J. Biometeorol.,* **56,** 429–441, https://doi.org/10.1007/s00484-011-0424-7.

Gandin, L. S. and A. H. Murphy, 1992: Equitable skill scores for categorical forecasts. *Mon. Wea. Rev.,* **120,** 361–370, https://doi.org/10.1175/1520-0493(1992)120<0361:ESSFCF>2.0.CO;2.

Havenith, G., and Coauthors, 2012: The UTCI-clothing model. *Int. J. Biometeorol.,* **56,** 461–470, https://doi.org/10.1007/s00484-011-0451-4.

Heusinkveld, B. G., L. W. A. Hove van, C. M. J. Jacobs, G. J. Steeneveld, J. A. Elbers, E. J. Moors, and A. A. M. Holtslag 2010: Use of a mobile platform for assessing urban heat stress in Rotterdam. *Proc. 7th Conf. on Biometeorology,* Freiburg, Germany, 433–438.

——, G. J. Steeneveld, L. W. A. vanHove, C. M. J. Jacobs, and A. A. M. Holtslag, 2014: Spatial variability of the

Rotterdam urban heat island as influenced by urban land use. *J. Geophys. Res.–Atmos.,* **119,** 677–692, https://doi.org/10.1002/2012JD019399.

Lindberg, F., B. Holmer, and S. Thorsson, 2008: SOLWEIG 1.0—Modelling spatial variations of 3D radiant fluxes and mean radiant temperature in complex urban settings. *Int. J. Biometeorol.,* **52,** 697–713, https://doi.org/10.1007/s00484-008-0162-7.

Matzarakis, A., F. Rutz, and H. Mayer, 2007: Modelling radiation fluxes in simple and complex environments—Application of the RayMan model. *Int. J. Biometeorol.,* **51,** 323–334, https://doi.org/10.1007/s00484-006-0061-8.

McCarthy, M. P., M. J. Best, and R. A. Betts, 2010: Climate change in cities due to global warming and urban effects. *Geophys. Res. Lett.,* **37,** L09705, https://doi.org/10.1029/2010GL042845.

Molenaar, R. E., B. G. Heusinkveld, and G. J. Steeneveld, 2016: Projection of rural and urban human thermal comfort in The Netherlands for 2050. *Int. J. Climatol.,* **36,** 1708–1723, https://doi.org/10.1002/joc.4453.

Oke, T. R., 1982: The energetic basis of the urban heat island. *Quart. J. Roy. Meteor. Soc.,* **108,** 1–24.

Osczevski, R., and M. Bluestein, 2005: The new wind chill equivalent temperature chart. *Bull. Amer. Meteor. Soc.,* **86,** 1453–1458, https://doi.org/10.1175/BAMS-86-10-1453.

Ronda, R. J., G. J. Steeneveld, J. J. Attema, B. G. Heusinkveld, and A. A. M. Holtslag, 2017: Urban fine-scale forecasting reveals weather conditions with unprecedented detail. *Bull. Amer. Meteor. Soc.,* **98**, 2675–2688, https://doi.org/10.1175/BAMS-D-16-0297.1.

Steadman, R. G., 1979: The assessment of sultriness. Part I: A temperature-humidity index based on human physiology and clothing science. *J. Appl. Meteor.,* **18,** 861–873, https://doi.org/10.1175/1520-0450(1979)018<0861:TAOSPI>2.0.CO;2.

Steeneveld, G. J., J. O. Klompmaker, R. J. Groen, and A. A. M. Holtslag, 2017: An urban climate assessment and management tool for combined heat and air quality judgements at neighbourhood scales. *Resour., Conserv. Recycl.,* in press.

Theeuwes, N. E., G. J. Steeneveld, R. J. Ronda, and A. A. M. Holtslag, 2017: A diagnostic equation for the daily maximum urban heat island effect for cities in northwestern Europe. *Int. J. Climatol.,* **37,** 443–454, https://doi.org/10.1002/joc.4717.

Weihs, P., H. Staiger, B. Tinz, E. Batchvarova, H. Rieder, L. Vuilleumier, M. Maturilli, and G. Jendritzky, 2012: The uncertainty of UTCI due to uncertainties in the determination of radiation fluxes derived from measured and observed meteorological data. *Int. J. Biometeor.,* **56,** 537–555, https://doi.org/10.1007/s00484-011-0416-7.

Wilks, D. S., 2006: *Statistical Methods in the Atmospheric Sciences: An Introduction*. Elsevier, 627 pp.

Zander, K. K., W. J. W. Botzen, E. Oppermann, T. Kjellstrom, and S. T. Garnett, 2015: Heat stress causes substantial labour productivity loss in Australia. *Nat. Climate Change,* **5,** 647–651, https://doi.org/10.1038/nclimate2623.

LOOKING FOR AN EXPERT?

LOOK TO AMS!

AMS announces the launch of our new online directory of
Weather and Climate Service Providers.

This new online directory, which will replace the former BAMS Professional Directory, will list an array of weather and climate service providers. You can find the new directory under the **"Find an Expert"** link from the AMS home page.

It's easier than ever for the weather, water, and climate community and the general public to search for organizations and individuals offering these important services.

Learn more at www.ametsoc.org

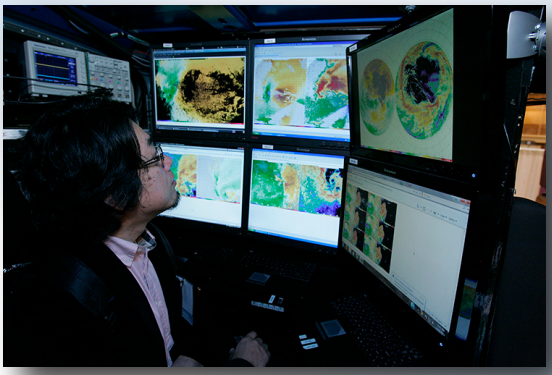

NEW!

Weather & Climate Service Providers Directory

AMS
American Meteorological Society

www.ametsoc.org